Adsorption of La³⁺ and Gd³⁺ Using magnetic iron oxide Nanoparticles: Mechanistic and Kinetic Study

Radwa M.Ashour[1], Ahmed A.Abdel-khalek[2], M.M.Ali[1], Ahmed F.Abdel-Magied[1]*

[1]Nuclear Material Authority, P. O. Box 530, El Maadi, Cairo, (EGYPT)
[2]Department of Chemistry, Faculty of Science, Beni-Sueif University, Beni-Sueif, (EGYPT)
E-mail: dr_ahmedfawzynma@yahoo.com

ABSTRACT

Magnetic iron oxide nanoparticles (MNPs) have been synthesized and fully characterized by using different spectroscopic techniques such as transmission electron microscopy (TEM), X-ray diffraction (XRD) and infrared spectra (FT-IR). The synthesized particles used as a friendly nanoadsorbent for adsorption trivalent rare earth ions RE^{3+} (La^{3+} and Gd^{3+}) from aqueous solution. The adsorption of La^{3+} and Gd^{3+} as a function of contact time, initial solution pH and temperature was investigated. Moreover, kinetics and thermodynamics were studied to understand the adsorption mechanism of La^{3+} and Gd^{3+} into the synthesized MNPs. The obtained thermodynamics functions ΔH, ΔS and ΔG reveal that sorption is thermodynamically driven. In addition, the adsorbed La^{3+} and Gd^{3+} can be readily desorbed 99% from the MNPs surface by using 0.5 M nitric acid.
© 2016 Trade Science Inc. - INDIA

INTRODUCTION

Rare earth (RE) elements are a group of chemical elements that includes all the lanthanides, yttrium and scandium. Given their particular spectroscopic and magnetic properties, the RE elements play an important role in many fields of advanced materials science; therefore, industrial demand for them has increased[1], such as magnet, electronics, super conductors, medical and nuclear technologies[2]. They are "rare" because they do not naturally occur in metallic form, only as mixed and scattered in minerals and are difficult to separate from each other due to very similar physico-chemical properties, which explains why the history of their discovery has a long period[3,4]. Therefore, separation, sorption and recovery of lanthanide from nuclear and metal-containing industrial waste streams are important both environmentally and economically. The most widely used techniques for the separation and recovery of REEs include precipitation[5], liquid-liquid extraction[6], ion exchange[7] and adsorption[8,9]. In all the aforementioned literature, the lanthanide metals were successfully separated or adsorbed using supported materials as solid–liquid extraction and sorption method. Solid-liquid extraction technique (SPE) has become one of the most widely used for REEs separation, due to it is simple to implement, high preconcentration factor to be attained, rapid phase separation, and easily incorporated into automated analytical techniques[9,10]. The adsorbent has a crucial function in SPE-based methods because it determines the selectivity, affinity, and capacity. Ideal SPE adsorbents are expected to

Full Paper

have the following characteristics: (i) porosity, having a large specific surface area, (ii) low blank, (iii) high chemical and mechanical stability, (iv) fast kinetics of adsorption and desorption, (v) reversible adsorption, (vi) high selectivity and finally (vii) high recovery efficiency. Great efforts have been made in the investigation of novel materials for SPE technology, as revealed by the increasing number of publications describing new and more selective sorbents or procedure[4,11,12]. Several types of nanomaterials, including magnetic iron oxide nanoparticles (MNPs) have unique advantages SPE adsorbents such as favorable chemical stability, low cost, easily retrieved from solution with a magnet. Task specific magnetic nanoparticles can be prepared by coating the surface with functional groups[13].

In this work, we focused on the development of SPE method by using material in nano-size such as iron-oxide nanoparticles for adsorption of our target metal ions $RE^{3+} = La^{3+}$ and Gd^{3+} from aqueous solution. In order to confirm the successful synthesis of the synthesized Fe_3O_4 magnetic nanoparticles, full characterization including TEM, XRD, FTIR and zeta potential have been carried out. In batch adsorption tests, different parameters were evaluated such as loading capacity, adsorption kinetics, thermodynamics parameters and influence of pH. Desorption and recovery of RE^{3+} ions from MNPs at different concentrations using different eluent concentration was also carried out. Adsorption isotherm, kinetics and mechanistic studies have been carried out.

MATERIALS AND METHODS

Material

All the chemicals used in this study were of analytical grade and used without further purification. High purity $La(NO_3)_3 \cdot 6H_2O$ (99.9%) and $Gd(NO_3)_3 \cdot 6H_2O$ (99.9%), sulfuric acid (96%), ferric chloride hexahydrate ($FeCl_3 \cdot 6H_2O$, $\geq$ 99%), ferrous chloride tetrahydrate ($FeCl_2 \cdot 4H_2O \geq$ 98%), ammonium hydroxide (25%), standard of La^{3+} and Gd^{3+} solutions (1000 mg/L in 2% HNO_3), nitric acid (65%) and sodium hydroxide (98%) were purchased from Sigma Aldrich. All reagents used in the study were of analytical grade and their respective solutions were prepared with

distilled water.

Characterization

Inductively coupled plasma-Optical Emission Spectroscopy (ICP-OES), (Thermo scientific iCAP6500 series) to determine the concentrations of metal ions. The operation conditions were carried out by adjustment of solutions pH using pH-meter (ORION 410 A). Ultrasonic vibration was applied to prepare MNPs dispersion. X-ray powder diffraction was performed on a Phillips X'Pert pro super diffract meter with Cu Ka (k= 1.5418 Å), Transmitted electronic microscopy (TEM), A Fourier transform infra-red (FTIR), (Nicolet Instruments model Avatar-100 equipped with ATR diamond at 303 K, Madison, WI, USA) and the zeta potential (Delsa Nano C, Beckman Coulter, Brea, CA, USA).

Synthesis of iron oxide MNPs

Iron oxide nanoparticles was prepared by co-precipitation method. Generally, 1.988 g (0.125 mol) of $FeCl_2 \cdot 4H_2O$ and 5.406 g (0.25 mol) of $FeCl_3 \cdot 6H_2O$ (1:2) molar ratio are dissolved in 80 mL water in a round flask and temperature was slowly increased to 70 °C under nitrogen atmosphere with mechanical stirring at 370 rpm for 30 min then 20 ml of ammonium hydroxide solution (25%) was added instantaneously to the reaction mixture and kept the reaction for another 30 min at 70 °C. The obtained black precipitates were washed with water three times and separated from the supernatant using a permanent magnet to get iron oxide MNPs.

Batch SPE experiments

Stock solutions of lanthanum nitrate $(La(NO_3)_3 \cdot 6H_2O)$ and $(Gd(NO_3)_3 \cdot 6H_2O)$ were prepared by dissolving an appropriate amount in deionized water. In a typical adsorption experimental process, 2.5 mg of MNPs mixed with 10 mL of mixture solution of La^{3+} and Gd^{3+} in batch reactor was placed in the constant-temperature shaker with speed 70 rpm. The pH was adjusted to the desired condition range from 3 to 8. Adsorption kinetics studies of RE^{3+} ions were carried out at the same condition but varying of contact time from 1 to 120 min. The initial concentration of RE^{3+} sample was varied from 5 to 50 ppm. In order to investigate the thermodynamic parameters carried

Full Paper

out by changing on adsorption temperature ranged from 278 to 318 K. Desorption of La^{3+} and Gd^{3+} from MNPs using different concentration of HNO_3 as eluent was carried out. Finally, magnetic nanoadsorbents were separated from mixture with an external magnet and ultracentrifuge with speed 10.000 rpm. The adsorption capacity (q_e) of La^{3+} and Gd^{3+} were calculated by equation (1).

$$\text{Adsorption capacity } (q_e) = \frac{(C_i - C_e)V}{m} \quad (1)$$

where C_i is the initial RE^{3+} concentration (mg/L), C_e is the equilibrium RE^{3+} concentration (mg/L) in the aqueous solution, V is the total aqueous volume (ml) and m is the mass of MNPs (mg).

Adsorption kinetics

The adsorption kinetics is great importance for adsorption investigation because they can indicate the adsorption rate of the RE^{3+} from solutions and supply effective data for comprehending the mechanism of adsorption reactions[14,15]. Herein, the adsorption kinetics was analyzed using the linear forms of pseudo-first-order and pseudo-second-order models; equations 3 and 4 were applied to investigate the adsorption mechanism.

$$\ln(q_e - q_t) = \ln q_e - k_1 t \quad (3)$$

$$\frac{t}{q_t} = \frac{1}{k_2 q_e^2} + t/q_e \quad (4)$$

where k_1 (min^{-1}) is the rate constant for first – order adsorption, k_2 (g/mgmin) is the rate constant for second-order adsorption, q_e (mg/g) is the adsorption capacity at equilibrium and q_t (mg/g) is the adsorption capacity at any time t.

Desorption studies

To measure the desorption process of RE^{3+} ions on MNPs adsorbents, the preloaded RE^{3+}-MNPs adsorbents were prepared using the same procedure mentioned above. The amounts of the loaded RE^{3+} on MNPs adsorbent (C_{des}) were calculated by equation 5.

$$\text{Desorption } \% = \frac{C_{des}}{C_{ads}} \times 100 \quad (5)$$

where C_{des} is the amount of La^{3+} and Gd^{3+} released into aqueous solution (mg/l) and C_{ads} is the amount of La^{3+} and Gd^{3+} adsorbed on the coated MNP (mg/l).

RESULT AND DISCUSSION
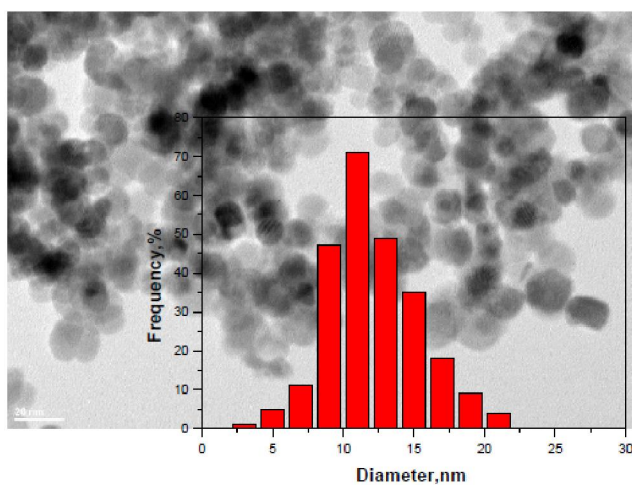
Iron oxide MNPs characterization

The typical TEM micrograph of the iron oxide MNPs was shown in Figure 1a. It was clear that the MNPs was essentially monodisperse and had a similar mean distribution size about (12 ± 3) nm. Additionally, no aggregation was observed, indicating the excellent dispersibility of MNPs in water. XRD pattern of the synthesized MNPs is presented in Figure 1b. Six characteristic peaks for Fe_3O_4 nanoparticles corresponding to (2 Theta) = 30.136, 35.554, 43.2, 53.529, 57.012, 62.961 and 89.690 for (220), (311), (400), (422), (511), (440) and (731) planes, respectively. These peaks are well matched with the magnetite characteristic peaks (JCPDS card no.19-0629) confirming the functionalized process did not result in the phase change and the magnetic nature of iron oxide MNPs was validated[16]. The FTIR spectra of the synthesized iron oxide MNPs were recorded. Figure 1c shows the FTIR spectra of the pristine Fe_3O_4. The analysis indicated absorption peaks at 584 cm^{-1} corresponding to the Fe–O vibration related to the magnetite phase. Further two bands around 3424 cm^{-1} and 1624 cm^{-1} ascribed to stretching and bending vibrations of surface hydroxyl groups, respectively[17].
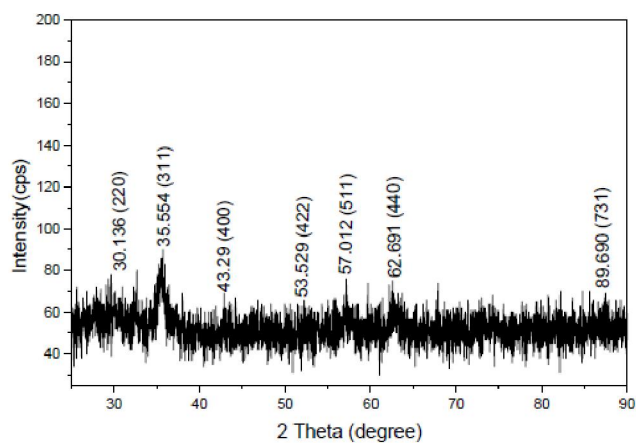
Batch adsorption studies

The synthesized iron oxide MNPs possess have a great potential in their applicability in heavy metal adsorption[18], so the feasibility of iron oxide MNPs as nanoadsorbent for removal of RE^{3+} ions from aqueous solution was demonstrated by using La^{3+} and Gd^{3+} ions as a target of REEs. The removal efficiency can be influenced by various factors as following:
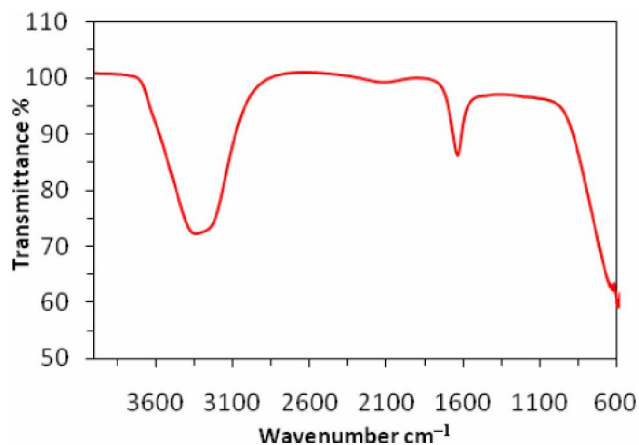
(a) Effect of contact time

The contact time between adsorbent and adsorbates is a vital parameter for evaluating the adsorption properties of adsorbents. Results of influence of contact time on the adsorption capacity are shown in Figure 2. Generally, adsorption is a time-consuming process; the indicating contact time was beneficial for the sufficient loading of La^{3+} and Gd^{3+} ions on the adsorption sites of iron oxide MNPs. The obtained results show that the adsorption capacity increased sharply within 10 min and

(a)

(b)

(c)

Figure 1 : a) TEM image; b) XRD pattern and c) FT–IR of the synthesized iron oxide MNPs

reached to maximum equilibrium within 30 min. With the increase of contact time, more adsorption sites were occupied and reach to 12.1 mg/g and 16.2 mg/g of adsorption capacity for La^{3+} and Gd^{3+}, respectively. So, 30 min was enough to reach to adsorption capacity of
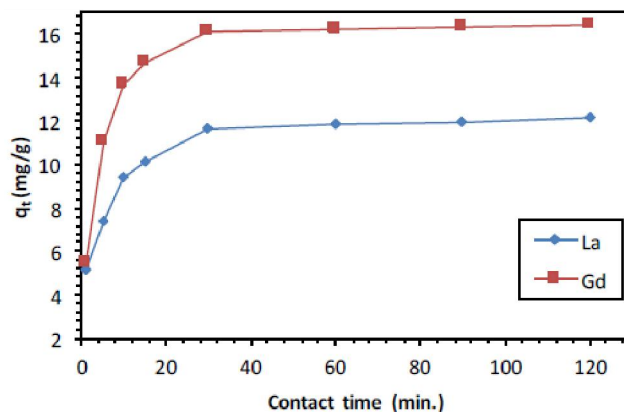

Figure 2 : Effect of contact time on the adsorption capacity of La^{3+} and Gd^{3+}. Experiment conditions: sample pH = 7; volume of sample = 10 mL; concentration of iron oxide MNP = 2.5 mg at room temperature
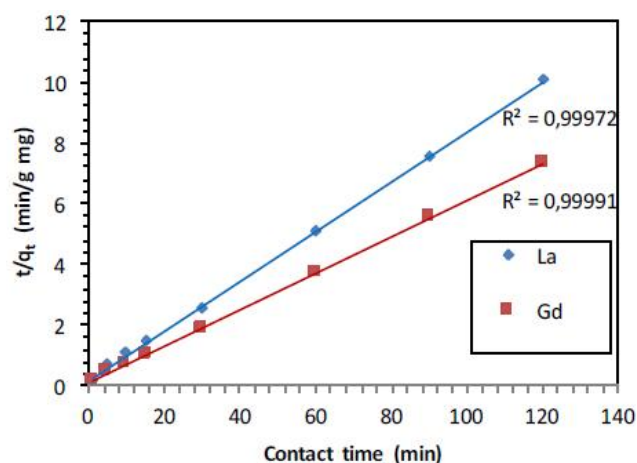

Figure 3 : Pesudo-second order kinetic model for the adsorption of La^{3+} and Gd^{3+} with iron oxide MNPs

TABLE 1 : Coefficients of pseudo-first-order and pseudo-second-order adsorption kinetic models

Kinetic model	Parameters	La^{3+}	Gd^{3+}
Pseudo-first order	K_1 (min^{-1})	0.02	0.03
	q_e (mg/g)	0.26	0.19
	R^2	0.763	0.866
Pseudo-second-order	K_2 (g/mg min)	0.03	0.01
	q_e (mg/g)	12.19	16.75
	R^2	0.999	0.999

RE^{3+}.

Adsorption kinetics, as an important aspect of adsorption mechanism study, were investigated by following linear of pseudo-first order and pseudo-

Full Paper

second order models[19]. The kinetics results are represented in Figure 3 and the calculated results were listed in TABLE 1. The correlation coefficient R^2 of the pseudo-first order kinetic model were all less than 0.763 and those of the pseudo-second order kinetic model were all more than 0.999, indicating better fitting to pseudo-second order kinetic model. The rate–limiting step may be chemical adsorption or chemisorption through sharing or exchange of electrons between adsorbents and adsorbates. In the initial 10 min, the adsorption capacity increased rapidly means that the chemical adsorption worked at fast rate[20].

(b) Effect of pH and zeta potential

To determine the experimental conditions at which La^{3+} and Gd^{3+} are effectively adsorbed with MNPs, the sorption studies have been carried out at different equilibrium pH levels. From iron oxide MNP synthesized, the surface of Carboxyl-MNPs functionalized with oxygen containing groups. Furthermore, S. Prijic and co-workers have
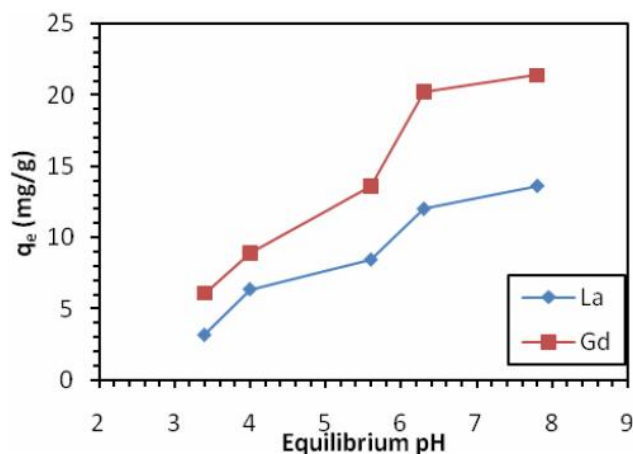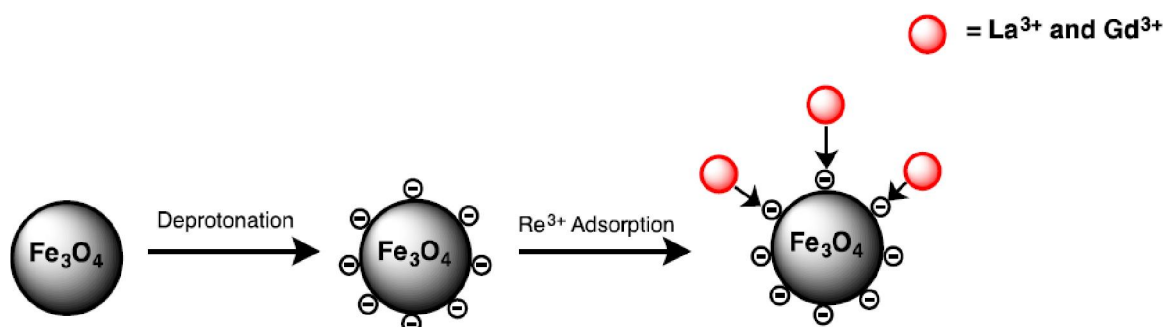

Figure 4 : Effect of sample pH on the adsorption capacity of La³⁺ and Gd³⁺. Experiment conditions:(contact time = 30 min, volume of sample =10 ml, conc. of MNPs = 2.5 mg at room temperature)

demonstrated that the isoelectric point of MNPs is at pH_{IEP} 6.1[21]. In order to to evaluate effect of pH, a series of sample solution are adjusted to a pH range of 3 to 8 and a process according to recommended procedure as represented in scheme 1. The adsorption capacities gently increase rapidly from 3.2 to 13.6 mg/g for La^{3+} and from 6 to 21 mg/g for Gd^{3+}. According to zeta potential results, the surface of MNP at low pH is positive charge due to the protonation of hydroxyl group ($—OH_2^+$) and a few amount of free (—OH). La^{3+} and Gd^{3+} are expected to exist predominantly in the RE^{3+} form. The adsorption capacity of La^{3+} and Gd^{3+} are very low because the electrostatic repulsion between RE^{3+} and positive charge on the surface of iron oxide MNPs and the concentration of H^+ increases with decreasing pH, which competes with La^{3+} and Gd^{3+} and makes the ion exchange reaction in the surface very difficult. At $pH > pH_{IEP}$ The adsorption capacity rises in the pH range of 6 to 8. A possible reason may be that the surface charge is negative charge from zeta potential results; isoelectric point (pH_{IEP}) is 6.1, due to deprotonation of hydroxyl group on the MNPs surface. So, the adsorption capacity increases because the electrostatic attraction between La^{3+} and Gd^{3+} and negative charge on the MNPs surface, the reaction carried out by ion exchange mechanism. The pH of 7.00 is selected in subsequent work[22]

Effect of temperature and thermodynamic parameters

In order to confirm the mechanism involved in the extraction process, we have investigated the influence of temperature on the adsorption capacity of La^{3+} and Gd^{3+} using iron oxide MNPs. The obtained results indicate that as the temperature increases from 278 to 318 K, the adsorption capacities of La^{3+} and Gd^{3+}

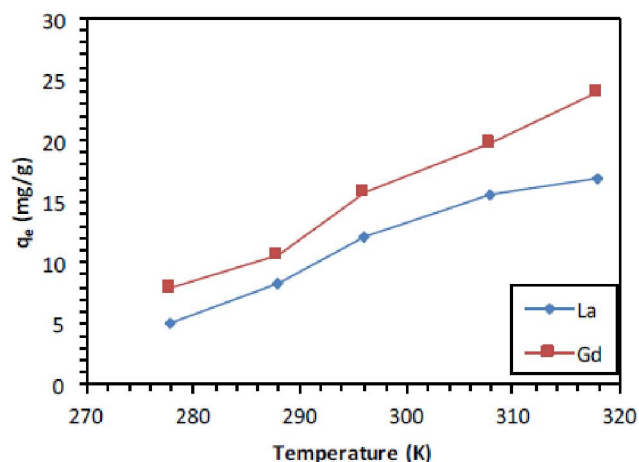**Scheme 1 : Schematic formation process of pH effect on adsorption**

Figure 5 : Effect of temperature on the adsorption capacity of La^{3+} and Gd^{3+}. Experiment conditions: sample pH = 7; volume of sample = 10 mL; concentration of MNPs = 2.5 mg
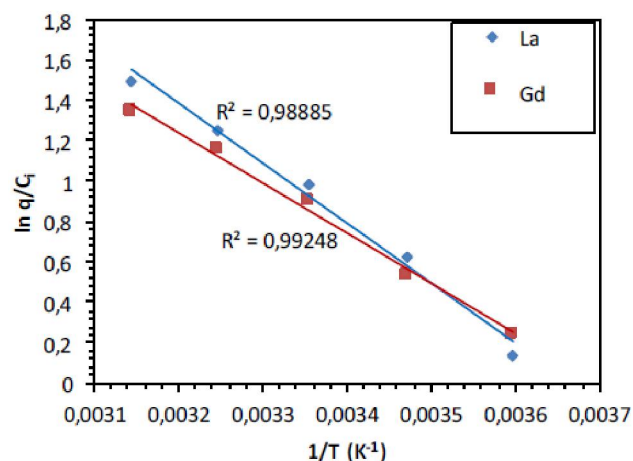
TABLE 2 : Thermodynamics parameters for adsorption efficiency of La^{3+}, Nd^{3+}, Gd^{3+} and Y^{3+} by iron oxide MNPs at different temperature

Temperature (K)	Parameters	La^{3+}	Gd^{3+}
	$\Delta H°$ (KJ/mol)	28.75	23.75
278 K	$\Delta S°$ (J/mol K)	101.45	84.38
	$\Delta G°$ (KJ/mol)	−28.23	−23.41
	$\Delta H°$ (KJ/mol)	28.75	23.75
318 K	$\Delta S°$ (J/mol K)	101.45	84.38
	$\Delta G°$ (KJ/mol)	−32.33	−26.81

Figure 6 : Linear plot of ln K_d vs 1/T for the removal efficiency of La^{3+} and Gd^{3+} on iron oxide MNPs at 278, 298, 308 and 318 K
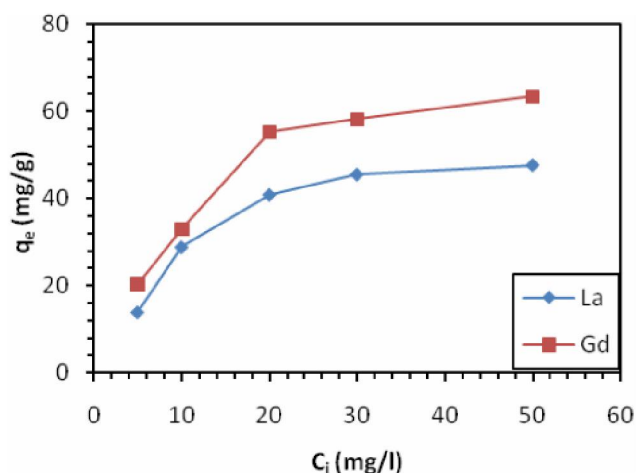

Figure 7 : Effect of initial concentration on the adsorption of La^{3+} and Gd^{3+} on MNPs. Experiment conditions: (pH = 7, iron oxide MNPs conc. =2.5 mg and contact time = 30 min at room temperature)

increase as represented in Figure 5. The results suggest that higher temperature is favourable to speeding La^{3+} and Gd^{3+} adsorption on iron oxide MNPs surface.

The thermodynamic parameters $\Delta H°$, $\Delta S°$ and $\Delta G°$ for La^{3+} and Gd^{3+} sorption on iron oxide MNPs can be calculated by using the following equations:

$$\ln K_d = -\frac{\Delta H°}{RT} + \frac{\Delta S°}{R} \tag{6}$$

$$\Delta G° = \Delta H° - T\Delta S° \tag{7}$$

where R (8.314 J/mol K) is the gas constant, T (K) is the temperature in Kelvin and K_d is the equilibrium constant. $\Delta H°$ (KJ/mol) is the enthalpy change, $\Delta S°$ (J/mol K) is the entropy change and $\Delta G°$ (K J/mol) is the Gibbs free energy change in a given process. The results of the thermodynamic parameters ($\Delta H°$, $\Delta S°$ and $\Delta G°$) are listed in TABLE 2. Linear plots of lnK_d versus 1/T

for La^{3+} and Gd^{3+} sorption on MNPs are shown in Figure 6. The thermodynamic parameters are calculated from the plot of lnK_d vs 1/T using equations 6 and 7. The positive values of $\Delta H°$ (K J/mol) indicates that the nature of adsorption and the removal efficiency of La^{3+} and Gd^{3+} on iron oxide MNPs is an endothermic process, and it would be increase with increase of temperature. The positive $\Delta S°$ values, also indicates that the sorption process is spontaneous with high affinity. The negative $\Delta G°$ values also indicates that the spontaneous process for removal efficiency of RE^{3+} on iron oxide MNPs under the conditions applied. The decrease of $\Delta G°$ with increasing temperature indicates more removal efficiency at higher temperature, RE^{3+} ions are readily dehydrated, and therefore the adsorption or removal

Full Paper

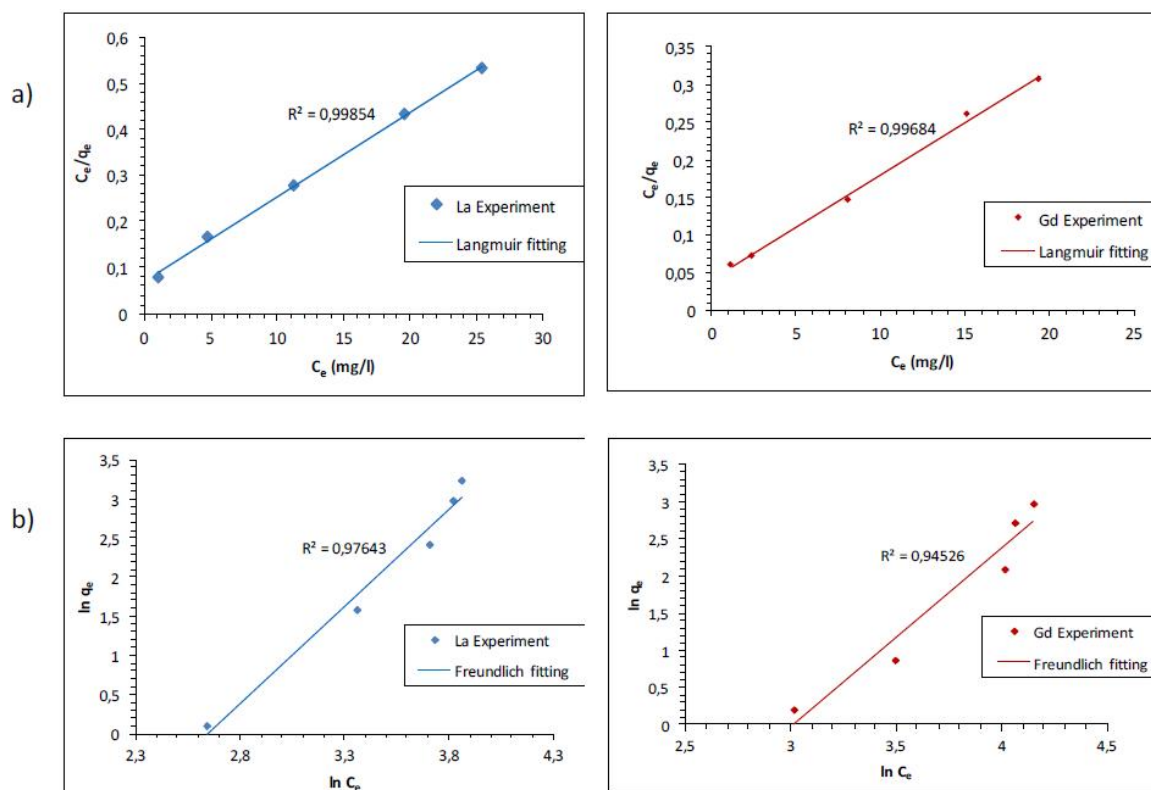**Figure 8 : Adsorption isotherms of La³⁺ ions on MNPs according to Langmuir equation (A) and Freundlich equation (B). Experiment conditions: (pH = 7; contact time and 30 min at room temperature)**

efficient becomes more favorable.

Adsorption isotherm

In order to illustrate the interaction between adsorbates and adsorbent, the effect of initial concentration on the adsorption capacity of iron oxide MNPs. The results indicated that the adsorption capacity of La³⁺ and Gd³⁺ increased with increasing initial concentration from 5 mg/L to 30 mg/L and then tended to level off. The result is probably due to the increase in the driving force of concentration gradient and the concentration at the adsorbent–adsorbates interface with an increase in the initial concentration as shown in Figure 7. When the active sites on the adsorbents are occupied sufficiently, the adsorption is saturated, and the adsorption capacity reaches a maximum level.

The maximum adsorption capacity of La³⁺ and Gd³⁺ at equilibrium isotherm adsorption data have been analyzed by Langmuir and Freundlich isotherm models, which are most popular isotherm theories:

$$C_e/q_e = C_e/q_{max} + 1/bq_{max} \tag{1}$$

where qe is the amount of RE³⁺ ions adsorbed on iron oxide MNPs at adsorption equilibrium (mg/g), Ce is

the equilibrium RE³⁺ ions concentration in solution (mg/L), qmax represents the maximum uptake of the RE³⁺ ions (mg/g) and b is the Langmuir constant (L/mg), related to the binding energy of adsorption (affinity), respectively. A plot of C_e/q_e versus C_e yields a straight line with a slope of $1/q_{max}$ and intercept of $1/bq_{max}$ as shown in Figure 8A. According to the slope and intercept of the fitted line, the value of q_{max} and b can be calculated, as summarized in Table 3. The value of the correlation coefficient R^2 for the Langmuir equation is 0.998, suggesting that the adsorption of La³⁺ and Gd³⁺ on iron oxide MNPs fitted the Langmuir equation isotherm very well.

The Freundlich isotherm is an empirical equation and usually was employed to describe the heterogeneous systems. The linear form of a Freundlich equation can be represented as follows:

$$\ln q_e = \ln K_f + 1/n \ln C_e \tag{2}$$

where K_f is the constant depicting adsorption capacity related to bond strength and the slope 1/n is a measure of the adsorption intensity or surface heterogeneity. The value of K_f and n can be determined from the linear plot of lnq$_e$ versus lnC$_e$ (as shown in Figure 8B).

TABLE 3 : Langmuir and Freundlich constants for the adsorption of La³⁺ and Gd³⁺ ions on MNPs

Adsorption isotherm	Parameters	La³⁺	Gd³⁺
	b (l/mg)	0.46	0.56
Langmuir	q_{max} (mg/g)	50.7	67.1
	R^2	0.998	0.996
	K_F (mg/g)		
Freundlich	n	0.41	0.42
	R^2	0.976	0.945

It was found that the value of the correlation coefficient R^2 estimated from the Langmuir equation was significantly higher than that calculated from Freundlich equation (TABLE 3). Thus, it can be concluded that the Langmuir equation gives a better fit to the experimental data than the Freundlich equation. Adsorption capacity of MNPs has been evaluated to be 50.7mg/g for La³⁺ and 67.1 mg/g Gd³⁺.

Desorption studies

Desorption performance is also an important nature for an adsorbent due to its influence on the potential practical application[23]. In this study, different concentration of HNO_3 (0.1–1M) was used as an eluent for elution/recovery operation of the absorbed REEs. The obtained results are represented in Figure 10. Firstly, the desorption experiments were first carried out using NaOH solutions and H_2O in which negligible amount of La³⁺ and Gd³⁺ was recovered. When HNO_3 solutions with different concentration were tested for the recovery
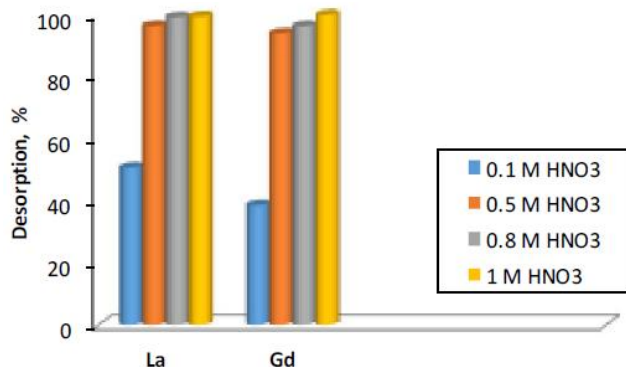

Figure 10 : Desorption of La³⁺ and Gd³⁺ from iron oxide MNPs using different HNO_3 concentrations (0.1–1M) for 30 min at 298 K

of RE³⁺ species from the loaded iron oxide MNPs, high recovery could be obtained. The data suggested that 0.5 M HNO_3 was suitable for complete recovery of ≈ 99% of La³⁺ and Gd³ from the surface of MNPs.

CONCLUSION

In this paper, a novel route for highly adsorption of La³⁺ and Gd³⁺ from aqueous solution by solid- phase extraction technique using iron oxide magnetic nanoparticle as a nanoadsorbent has been reported. At pH = 7 ± 0.1 and room temperature, MNPs achieve high adsorption capacities, 50.7 mg/g and 67.1 mg/g for La³⁺ and Gd³⁺, respectively. The kinetic data reveal that La³⁺ and Gd³⁺ sorption rate are fast. High desorption efficiency was obtained for the recovery of RE³⁺ ions by using HNO_3, where 0.5 M HNO3 was suitable for complete elution of adsorbed La³⁺ and Gd³⁺ from iron oxide MNPs.

REFERENCES

[1] T.S.Martins, P.C.Isolani; Terras raras: aplicações industriais e biológicas, Química Nova, **28**, 111-117 **(2005)**.

[2] E.Kim, K.Osseo-Asare; Aqueous stability of thorium and rare earth metals in monazite hydrometallurgy: Eh–pH diagrams for the systems Th–, Ce–, La–, Nd– (PO4)–(SO4)–H2O at 25 °C, Hydrometallurgy, **113–114**, 67-78 **(2012)**.

[3] F.Habashi; Extractive metallurgy of rare earths, Canadian Metallurgical Quarterly, **52**, 224-233 **(2013)**.

[4] G.A.Moldoveanu, V.G.Papangelakis; Recovery of rare earth elements adsorbed on clay minerals: I. Desorption mechanism, Hydrometallurgy, **117–118**, 71-78 **(2012)**.

[5] E.Fujimori, T.Hayashi, K.Inagaki, H.Haraguchi; Determination of lanthanum and rare earth elements in bovine whole blood reference material by ICP-MS after coprecipitation preconcentration with heme-iron as coprecipitant, Fresenius J.Anal.Chem, **363**, 277-282 **(1999)**.

[6] S.Tong, N.Song, Q.Jia, W.Zhou, W.Liao; Solvent extraction of rare earths from chloride medium with mixtures of 1-phenyl-3-methyl-4-benzoyl-pyrazalone-5 and sec-octylphenoxyacetic acid, Sep.Purif.Technol., **69**, 97-101 **(2009)**.

Full Paper

[7] Q.Jia, X.Kong, W.Zhou, L.Bi; Flow injection on-line preconcentration with an ion-exchange resin coupled with microwave plasma torch-atomic emission spectrometry for the determination of trace rare earth elements, Microchemical Journal, **89**, 82-87 **(2008)**.

[8] X.Sun, B.Peng, Y.Ji, J.Chen, D.Li; The solid–liquid extraction of yttrium from rare earths by solvent (ionic liquid) impreganated resin coupled with complexing method, Sep.Purif.Technol., **63**, 61-68 **(2008)**.

[9] J.Roosen, K.Binnemans; Adsorption and chromatographic separation of rare earths with EDTA- and DTPA-functionalized chitosan biopolymers, J.Mater.Chem.A, **2**, 1530-1540 **(2014)**.

[10] S.Babel, T.A.Kurniawan; Low-cost adsorbents for heavy metals uptake from contaminated water: a review, J.Hazard. Mater., **97**, 219-243 **(2003)**.

[11] P.Turan, M.Doğan, M.Alkan; Uptake of trivalent chromium ions from aqueous solutions using kaolinite, J.Hazard. Mater., **148**, 56-63 **(2007)**.

[12] P.Puig, F.Borrull, M.Calull, C.Aguilar; Recent advances in coupling solid-phase extraction and capillary electrophoresis (SPE–CE), Trends Anal. Chem., **26**, 664-678 **(2007)**.

[13] R.Hao, R.Xing, Z.Xu, Y.Hou, S.Gao, S.Sun; Synthesis, Functionalization, and Biomedical Applications of Multifunctional Magnetic Nanoparticles, Adv. Mater., **22**, 2729-2742 **(2010)**.

[14] V.Štengl, J.Bludská, F.Opluštil, T.Němec; Mesoporous titanium–manganese dioxide for sulphur mustard and soman decontamination, Materials Research Bulletin, **46**, 2050-2056 **(2011)**.

[15] G.Zhao, T.Wen, X.Yang, S.Yang, J.Liao, J.Hu, D.Shao, X.Wang; Preconcentration of U(vi) ions on few-layered graphene oxide nanosheets from aqueous solutions, Dalton Trans., **41**, 6182-6188 **(2012)**.

[16] J.Sangeetha, J.Philip; Synthesis, characterization and antimicrobial property of Fe3O4-Cys-HNQ nanocomplex, with l-cysteine molecule as a linker, Rsc.Adv., **3**, 8047-8057 **(2013)**.

[17] Y.L.Mikhlin, A.V.Kuklinskiy, N.I.Pavlenko, V.A.Varnek, I.P.Asanov, A.V.Okotrub, G.E.Selyutin, L.A.Solovyev; Spectroscopic and XRD studies of the air degradation of acid-reacted pyrrhotites, Geochimica et Cosmochimica Acta., **66**, 4057-4067 **(2002)**.

[18] X.Shen, Q.Wang, W.Chen, Y.Pang; One-step synthesis of water-dispersible cysteine functionalized magnetic Fe3O4 nanoparticles for mercury(II) removal from aqueous solutions, Appl Surf Sci., **317**, 1028-1034 **(2014)**.

[19] Y.Yao, S.Miao, S.Liu, L.P.Ma, H.Sun, S.Wang; Synthesis, characterization, and adsorption properties of magnetic Fe3O4@graphene nanocomposite, Chem.Eng.J., **184**, 326-332 **(2012)**.

[20] S.Yusan, C.Gok, S.Erenturk, S.Aytas; Adsorptive removal of thorium (IV) using calcined and flux calcined diatomite from Turkey: Evaluation of equilibrium, kinetic and thermodynamic data, Appl. Clay Sci., **67–68**, 106-116 **(2012)**.

[21] S.Prijic, J.Scancar, R.Romih, M.Cemazar, V.B.Bregar, A.Znidarsic, G.Sersa; Increased Cellular Uptake of Biocompatible Superparamagnetic Iron Oxide Nanoparticles into Malignant Cells by an External Magnetic Field, The Journal of Membrane Biology., **236**, 167-179 **(2010)**.

[22] S.Singh, K.C.Barick, D.Bahadur; Surface engineered magnetic nanoparticles for removal of toxic metal ions and bacterial pathogens, J.Hazard.Mater., **192**, 1539-1547 **(2011)**.

[23] M.R.Awual, T.Kobayashi, H.Shiwaku, Y.Miyazaki, R.Motokawa, S.Suzuki, Y.Okamoto, T.Yaita; Evaluation of lanthanide sorption and their coordination mechanism by EXAFS measurement using novel hybrid adsorbent, Chem. Eng. J., **225**, 558-566 **(2013)**.